EUCALL

The European Cluster of Advanced Laser Light Sources

Grant Agreement number: 654220

Work Package 4 – SIMEX

Deliverable D4.3

Interoperability of simulation workflows

Lead Beneficiary: European XFEL

Carsten Fortmann-Grote, Alexander Andreev, Richard Briggs, Michael Bussmann, Marco Garten, Axel Hübl, Thomas Kluge, Sakura Pascarelli, Ashutosh Sharma, Sergey Yakubov, and Adrian P. Mancuso

Due date: 30 September 2017
Date of delivery: 29 September 2017

Project webpage: www.eucall.eu

Deliverable Type	
R = Report DEM = Demonstrator, pilot, prototype, plan designs DEC = Websites, patents filing, press & media actions, videos, etc. OTHER = Software, technical diagram, etc.	R
Dissemination Level	
PU = Public, fully open, e.g. web CO = Confidential, restricted under conditions set out in Model Grant Agreement CI = Classified, information as referred to in Commission Decision 2001/844/EC	PU

This project has received funding from the *European Union's Horizon 2020 research and innovation programme* under grant agreement No 654220

Contents

This project has received funding from the *European Unions Horizon 2020 research and innovation programme* under grant agreement No 654220.

Abstract

We report five documented examples demonstrating the interoperability of simulation workflows in SIMEX. A first usage example has been presented in Milestone M4.2 [20].

1 Introduction

The following examples demonstrate the functionality and interoperability of all simulation tools as demanded in Task 4.2.2.:

1. Simulation of diffraction of coherent x–rays delivered by an X–ray Free–Electron Laser (XFEL) from high energy density matter created by short–pulse laser matter interaction (as detailed in Deliverable D4.1)
2. Simulation of XAFS from long–pulse laser shocked warm dense matter at the synchrotron light source ESRF (as detailed in Deliverable D4.2).
3. Coherent diffraction imaging of protein crystals
4. X–ray Thomson Scattering from warm dense plasmas
5. Laser–wakefield acceleration based coherent light sources

Table 1 summarizes the available simulation modules, the interfaced backengine simulation codes, and the relevant sections of this report and external references where example applications can be found.

Table 1: Demonstrated simulation capabilities

Task	Simulation capability	Simulation code	Example references
X–ray sources	XFEL source XFEL source Synchrotron source	FAST/XPD Genesis/Ocelot ShadowOUI	Refs [21, 20, 1] Sec. 6 Sec. 3
Beam propagation	Coherent wave propagation X–ray tracing	WPG/SRW ShadowOUI	Refs [21, 20, 1] Sec. 3
Photon–matter interaction	Radiation damage to molecules Short–pulse optical laser Long–pulse optical laser	XMDYN/XATOM PIConGPU Esther Rad–Hydro	Refs [21, 20, 1] Secs 6,2, Ref. [22] Sec. 3 Ref. [2]
Signal generation	Nano-particle scattering Plasma diffraction XAFS Plasma XRTS Nano–crystallography	singFEL paraTAXIS FEFF XRTScode CrystFEL	Ref. [21, 20, 1] Sec. 2,Ref. [22, 3, 26] Sec. 3, Refs [23, 2, 4, 5] Sec. 5, Ref. [6] Sec. 4

User interfaces for the simulation codes, as well as data interfaces and file format converters are implemented in the simulation environment *simex_platform*. Version 0.3.3 [7] of the software was released on September 22, 2017 in fulfillment of Milestone M4.3 [24].

2 Coherent diffraction from high energy density matter

The interaction of Ultra–High Intensity (UHI) lasers with solid matter at laser pulse durations of few ten to hundred femtoseconds opens up the possibility to study transient, non–equilibrium

This project has received funding from the *European Unions Horizon 2020 research and innovation programme* under grant agreement No 654220.

high energy density plasma processes on time scales close to that of atomic processes with XFELs with nanometer resolution [3], see also SIMEX Deliverable D4.1 [22]. Thus, radiation transport calculations must take these time and length scales into account. We here introduce the example of softening and expansion of a grating structure, see Fig. 1, that is irradiated by an UHI optical laser pulse to illustrate the possibilities of *ParaTAXIS*, a tool developed within WP4 that resolves radiation transport on the single photon level. *ParaTAXIS* is fully integrated into the *simex_platform* tool chain via *openPMD* [27] in- and output, see Fig. 2.

We study a $\tau_{\mathrm{opt}} = 83\,\mathrm{fs}$ full width at half maximum (FWHM) duration, wavelength $\lambda_{\mathrm{opt}} = 0.8\,\mu\mathrm{m}$ laser pulse impinging on a silicon foil under oblique incidence that drives the grating into a heated plasma state. An x–ray pulse of $\tau_{\mathrm{XFEL}} = 10\,\mathrm{fs}$ (FWHM) with photon energy $E_{\mathrm{XFEL}} = 8.4\,\mathrm{keV}$ probes the surface grating structure perpendicularly to the optical laser propagation with a delay relative to its pulse maximum arriving at the target surface. With growing delay we expect the scattering maxima of the grating to vanish as its edges soften and the plasma expands into the vacuum. The time structure of the XFEL pulse, the evolution of the target while the pulse probes it and effects like multiple-scattering smear out the scattering maxima. All effects are taken into account by *ParaTAXIS*. Details of the signal generation using *ParaTAXIS* for two cases (optically thin and optically thick target) are presented in the Deliverable Report D4.4 [25]. We show here the resulting scattering images in Fig. 3.

This project has received funding from the *European Unions Horizon 2020 research and innovation programme* under grant agreement No 654220.

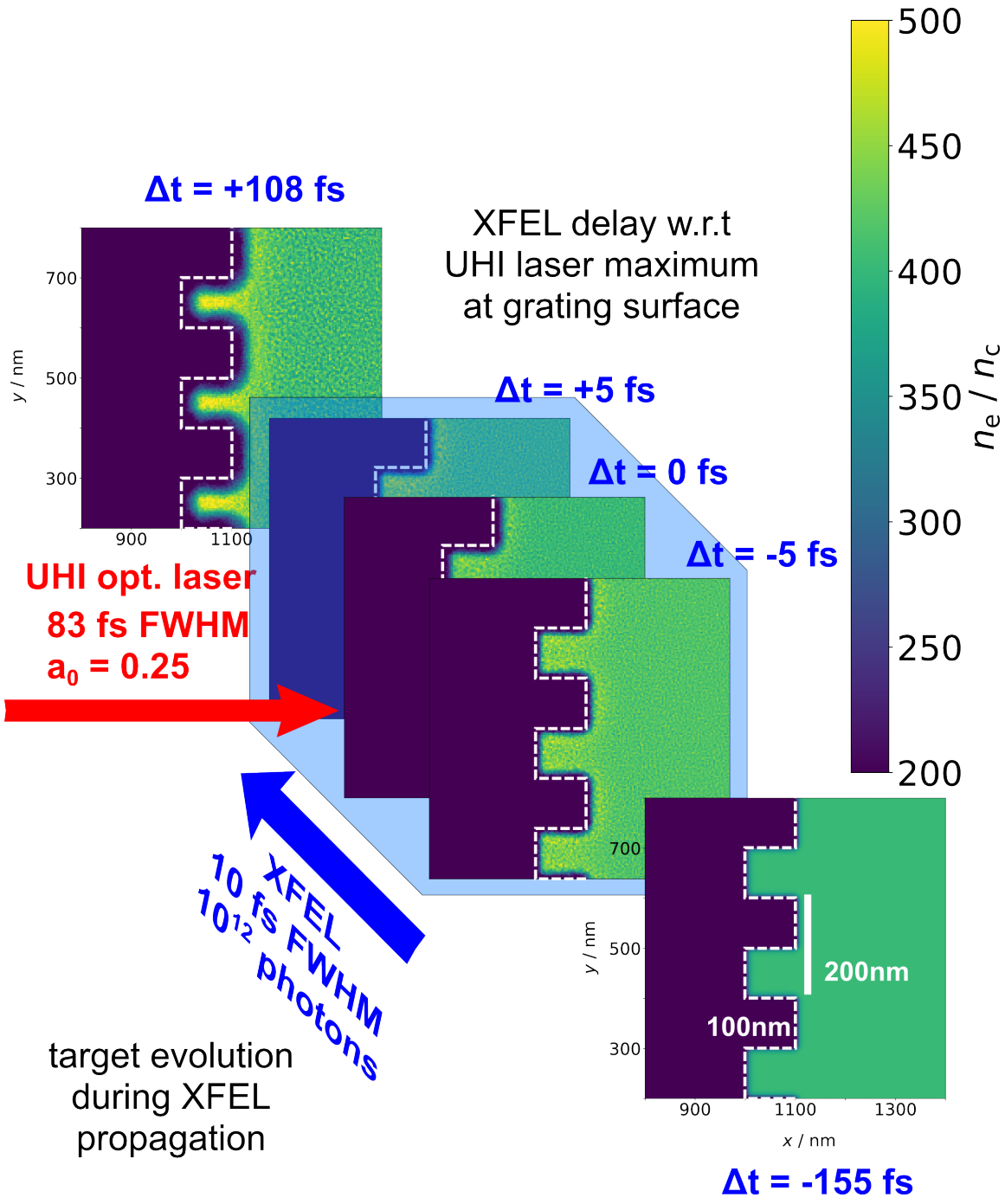

Figure 1: Scattering geometry with XFEL pulse perpendicular to optical UHI laser. The target is a silicon foil with a grating surface. As the XFEL pulse traverses the target, the electron density changes due to the UHI laser interacting with the grating which dissolves over time. Delay times of the XFEL pulse maximum are given with respect to the time when the optical laser pulse maximum hits the target surface. The area illuminated by the XFEL pulse is $2\lambda_{opt} \times 2\lambda_{opt}$, with the corresponding Small–Angle X–ray Scattering (SAXS) image, assuming 3 µm target depth, seen in Fig. 3.

This project has received funding from the *European Unions Horizon 2020 research and innovation programme* under grant agreement No 654220.

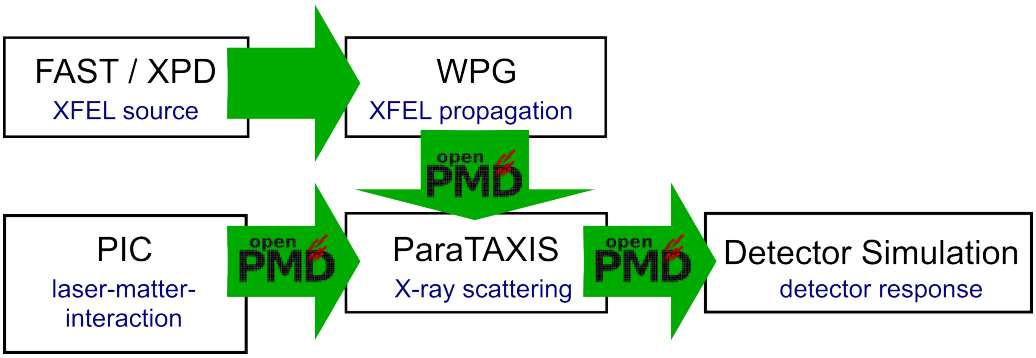

Figure 2: SIMEX workflow connecting the simulation codes via data exchange in *openPMD* standard.

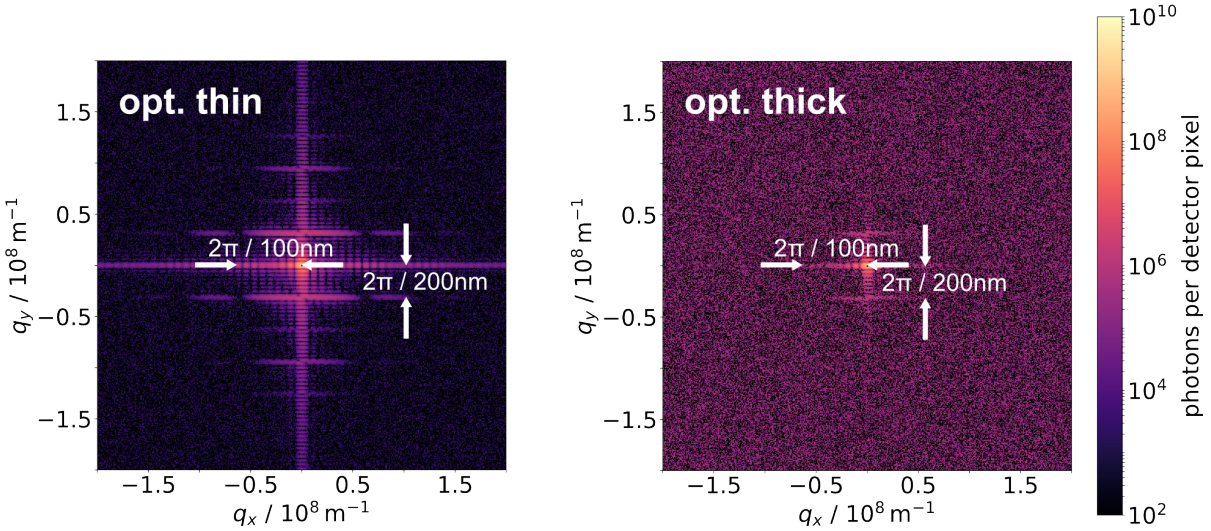

Figure 3: **Left:** *ParaTAXIS* SAXS image for the optically thin target at 1.4 m distance from the target, detector pixel size a_D = 13.5 µm, X-ray wavelength λ_{XFEL} = 1.47 Å and 10^{12} photons in the illuminated area. The vertical separation of scattering lines corresponds to the grating period of 200 nm, the horizontal to the grating depth of 100 nm. **Right:** *ParaTAXIS* SAXS image for the optically thick target. Here, the scattering cross section was increased by a factor of 1000 to account for resonant scattering at the ion density. All other parameters remain the same.

This project has received funding from the *European Unions Horizon 2020 research and innovation programme* under grant agreement No 654220.

3 XAFS

We have executed the simulations outlined in Deliverable 4.2[23], describing an XAFS experiment on shock compressed solid matter. There are three areas of simulation that are considered to describe the whole source-to-end experiment: X-ray source & ray tracing, long pulse photon-matter interaction, and X-ray absorption modelling. Currently, the simulations of X-ray source/X-ray tracing and XAS modelling are standalone simulations that provide important information for the long pulse hydrocode simulations. Information such as X-ray beam size on sample, will influence the laser conditions that can be accepted for hydrocode simulation (the laser spot must be larger than the X-ray spot size).

3.1 Synchrotron x–ray source and ray tracing

The synchrotron x–ray source and propagation from the source to the target is realized with the *Oasys* software package using the x–ray tracing code *Shadow3*. Installation scripts and the wiki page for *Oasys* can be found at https://github.com/srio/oasys-installation-scripts/wiki. Tutorials for Oasys and ShadowOUI cover the various steps in preparing, executing, and analysing the raytracing simulation. As part of preparation for the new High Power Laser Facility (HPLF), that will be installed on the ID24 beamline at the ESRF, the current energy dispersive x–ray absorption beamline has been simulated using *Oasys*. The ID24 beamline workflow for *Oasys* can be obtained from the EUCALL Data Repository at Zenodo [28].

3.2 Particle matter interaction: long pulse laser

The long pulse laser interaction with the sample is performed using the radiation–hydrodynamics simulation code *Esther* [8]. Here we have demonstrated an experiment that could be performed on the ID24 x–ray absorption spectroscopy (XAS) beamline, where a 6 ns flat top laser pulse (wavelength 1064 nm) sends an ablative driven shockwave through a 45 µm CH-plastic ablator and into a 5 µm Fe layer. A tutorial that describes how the input files are generated (and how output data is obtained) is provided on the *simex_platform* wiki page; all example input and output files are available from the Ref. [29]. The pressure in the Fe sample at t = 8.9 ns (laser pulse begins at t = 0 ns) is shown in Fig. 4.

The pressure, temperature, density and velocity can all be obtained at any given time step from the output files that Simex converts to OpenPMD [27] format. Upon completion of the code, it is then possible to adjust the laser parameters to reach different pressure-temperature conditions in the Fe sample. The P-T condition where the pressure is uniform through the whole of the sample is then recorded and XAS modelling can be performed to simulate the expected EXAFS signal at the compressed state.

3.3 Modelling of EXAFS

In this example, to show the interoperability with the hydrocode, we run through the requirements that are necessary for simulation (fitting) of EXAFS data relevant to obtain signal from a 5 µm thick Fe foil. The simulation will be carried out for ambient conditions Fe foil; a future enhancement of SIMEX will take P-T conditions from hydrocode simulations before performing high-pressure XANES/EXAFS calculations.

This project has received funding from the *European Unions Horizon 2020 research and innovation programme* under grant agreement No 654220.

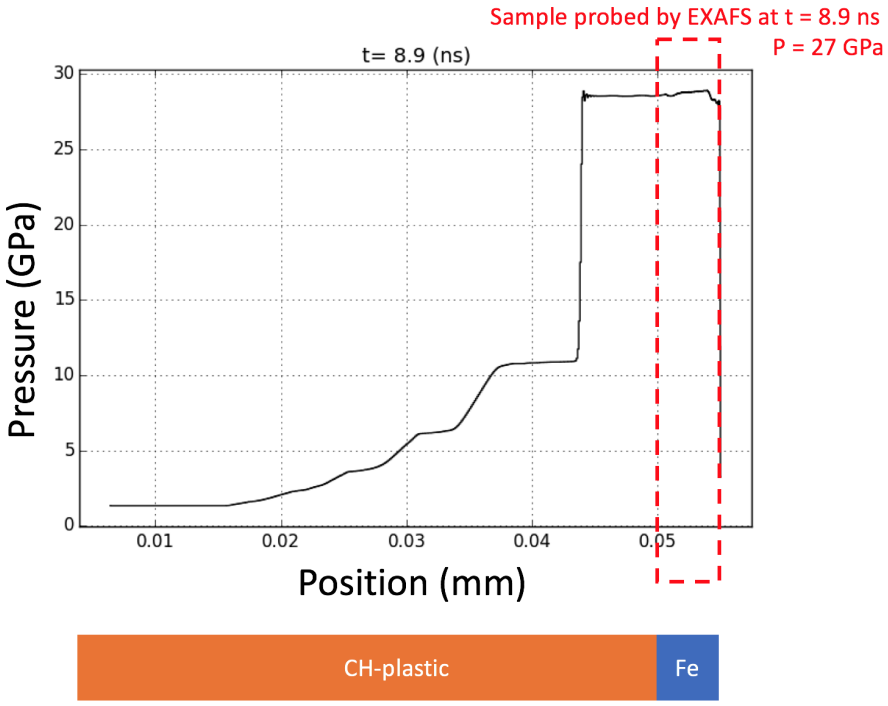

Figure 4: Pressure distribution in the plastic ablator layer (0-0.05 mm) and iron sample (0.05-0.055 mm). The laser arrives at 0 mm and sends the shock wave through the plastic. Upon reaching the Fe layer the shock pressure jumps to 30 GPa and sends a reshock wave back into the plastic. The red-dashed box highlights the iron sample that is probed by the X-rays.

This project has received funding from the *European Unions Horizon 2020 research and innovation programme* under grant agreement No 654220.

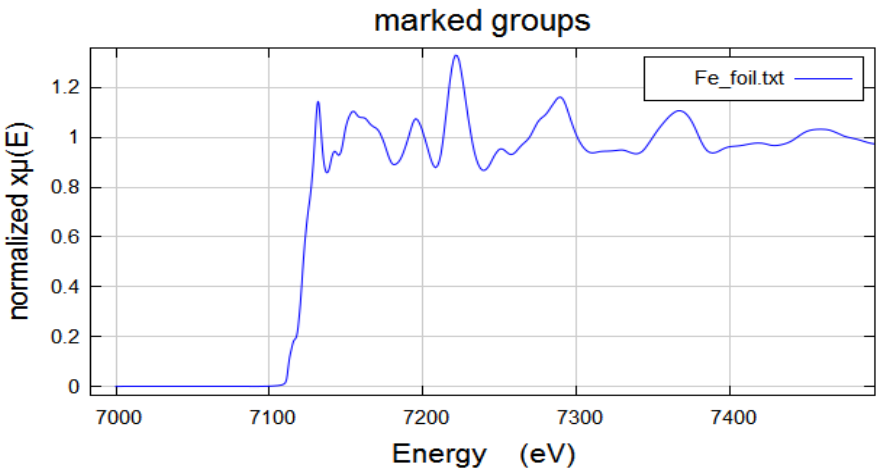

Figure 5: X–ray absorption spectra collected at BM23 (EXAFS beamline, ESRF) of a 5 µm thick iron foil.

To validate the EXAFS simulations, we compare the simulated spectrum with raw data obtained from an XAS beamline at the ESRF synchrotron. The normalized XAS spectrum for a 5 µm thick Fe foil is shown in Fig. 4. Calculations of XAFS spectra are performed using the *FEFF* package [9]. *FEFF* uses a single input file to select which modules should be run inside the program and what parameters should be used. The material of interest is contained within this input file based on its crystallographic parameters and atomic positions. The *ATHENA* program is able to combine crystallographic input files (.cif format) for a chosen material into the *FEFF* .inp format. The .cif files can be found on crystallographic database websites or can be manually created using gui programs such as *VESTA*. *FEFF* is then run to calculate the scattering paths between atoms and the run data is then exported for use by other third party programs (such as *ARTEMIS*) to compare with experimental data. A comprehensive user guide for running ARTEMIS / *FEFF* can be found at http://bruceravel.github.io/demeter/artug/index.html.

3.3.1 Simulating XANES at shock conditions

Shock compression experiments on Fe have previously been carried out at the ESRF [2]. In that study, simulations of the XANES at shock conditions were carried out using the *abinit* code and are shown below in Fig. 8.

A documented example workflow is provided to demonstrate the usability of the radiation–hydrodynamics simulation capabilities in *simex_platform*. It shows how to optimize the target geometry (i.e. the thickness of the ablator material) to maximize the data output, making use of the openPMD metadata standard to facilitate transferability among involved simulation codes and data analysis and visualisation tools.

This project has received funding from the *European Unions Horizon 2020 research and innovation programme* under grant agreement No 654220.

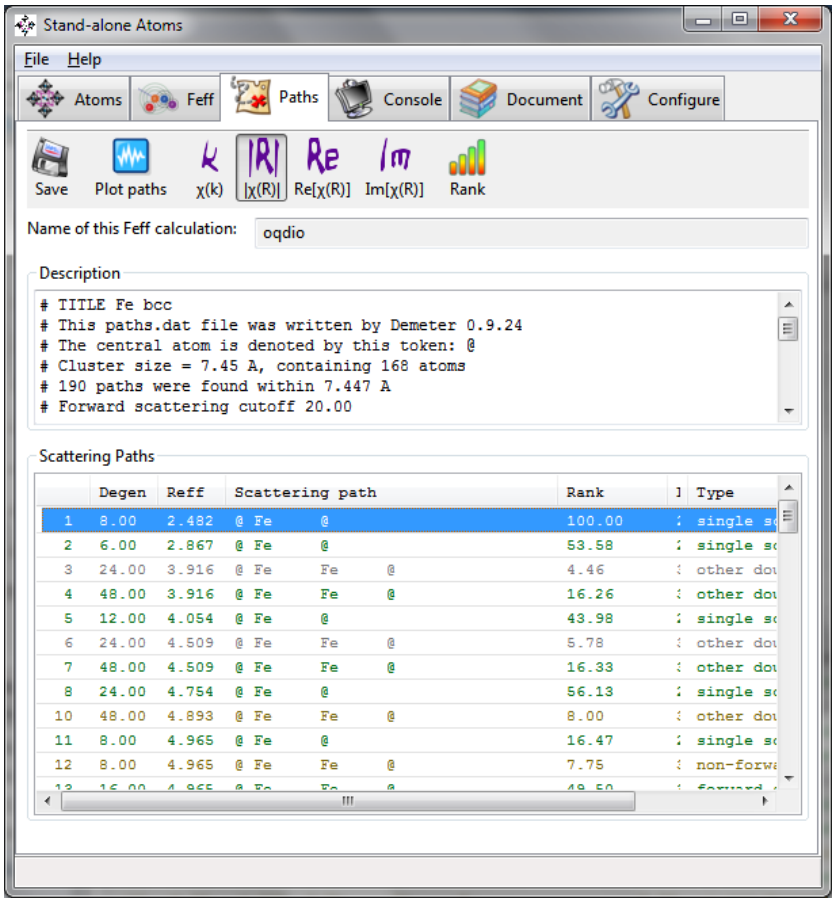

Figure 6: Screenshot of the output data collected in the ATOMS software after running *FEFF* simulation of iron at ambient conditions.

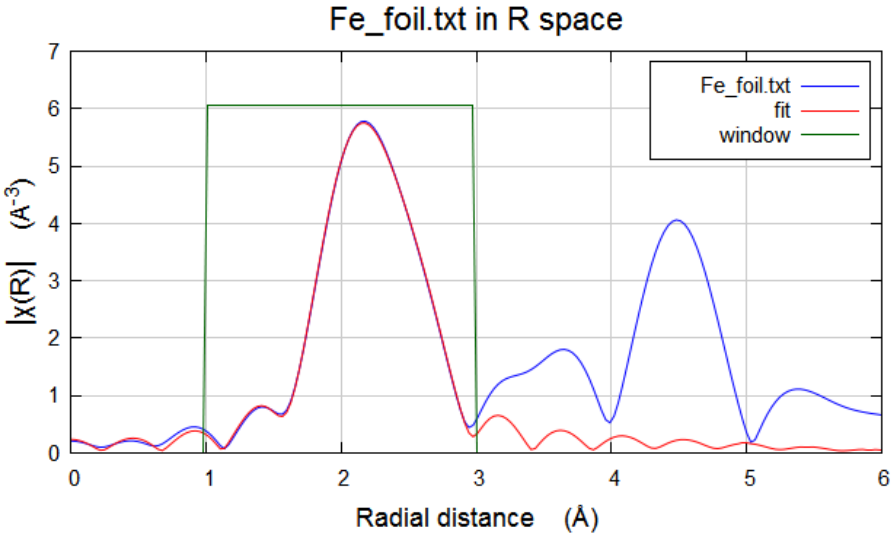

Figure 7: Fitting of the first Fe shell from *FEFF* calculations (red) to Fe EXAFS data collected on BM23 beamline, ESRF (blue).

This project has received funding from the *European Unions Horizon 2020 research and innovation programme* under grant agreement No 654220.

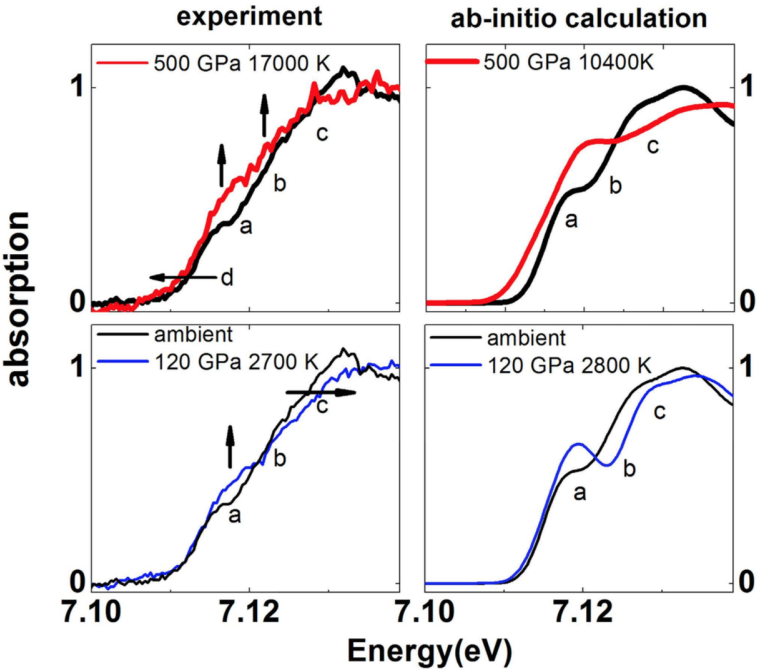

Figure 8: Comparisons of the absorption edge of Fe between experiments (left panels) and ab-initio calculations (right panels) at 120 GPa and 150 GPa. Figure taken from Ref. [2].

4 Coherent diffraction from protein nano–crystals

In an online tutorial, we demonstrate the usage of *simex_platform* to simulate coherent diffraction of XFEL photons from nano–metre scale crystalline samples. As in the other XFEL applications (see Sec. 2 and Sec. 5 as well as the first demonstration example in Milestone M4.2 [20]), the source wavefront is queried from the XFEL Pulses Database XPD and propagated to the sample interaction point in the focus of the SPB–SFX instrument by means of the coherent wavefront propagation code library WPG. Owing to the well defined data interfaces and file format adaptors in *simex_platform*, passing the wavefront data to the crystal diffraction code is straightforward. We employ the code *pattern_sim* which is part of the crystallography software suite *CrystFEL* [10], available as open source from the CrystFEL website. The corresponding *Calculator* in *simex_platform* is the *CrystFELPhotonDiffractor*. The *CrystFELPhotonDiffractor* extracts the mean photon energy, the energy spectrum, the beam divergence, the beam diameter, and other beam characteristics from the wavefront data. The sample must be specified by a PDB code along with information about the size of the nano–crystal, e.g. the extension in x,y, and z directions. By default, the sample geometry is rotated in space via a randomly chosen rotation operator to mimic the unknown orientation of the sample in the experiment. Each simulated pattern is stored in a separate hdf5 file. After the calculation, one master hdf5 file is generated which links to the individual patterns and which has the same hierarchy as output generated e.g. by the *SingFELPhotonDiffractor* for single particle coherent diffraction. This in turn ensures that the same visualization tools (e.g. *DiffractionAnalysis*) can be applied to crystal diffraction data and to single particle diffraction data.

This project has received funding from the *European Unions Horizon 2020 research and innovation programme* under grant agreement No 654220.

5 Plasma X–ray Thomson Scattering

X–ray Thomson Scattering (XRTS) [11, 6] has become an important method for the diagnosis of matter at extreme conditions of temperature and density. These quantities can be inferred from the spectrally resolved scattering intensity if the spectrum was measured with high resolution. The resolution primarily depends on the detector's point spread function, the energy resolution of the dispersive element, and on the spectral width of the probe radiation. Complex structured source spectra, e.g. K–shell multiplets [12] or saturated SASE (self–amplified spontaneous emission) spectra limit the accuracy to which plasma properties can be measured.

XRTS can now be simulated within *simex_platform*. The corresponding *Calculator* is the *PlasmaXRTSCalculator*, the backengine simulation code is called *xrs* and can be obtained by request from the maintainers of *simex_platform*. The *PlasmaXRTSCalculator* accepts wavefront data from the *XFELPhotonPropagator* from which it will extract the power spectrum of the scattering photons and convolute it with the dynamic structure factor coming from the *xrs* code.

A tutorial and example demonstration has been added to the *simex_platform* wiki. It explains how to setup the source, propagation and XRTS calculation to generate scattering spectra with explicit account for the source spectrum.

Fig. 9 demonstrates the impact of a broad SASE spectrum on the simulated XRTS spectrum. Here, we used a propagated wavefront from the SASE1 beamline at European XFEL of 3 fs duration and 5 keV photon energy. The simulation of the FEL source was performed at high saturation leading to the numerous SASE spikes and rather broad spectral width of the x–ray probe.

In Ref. [17], the theoretical models to describe scattering from weakly collisional plasmas implemented in *xrs* are benchmarked against a plasma kinetic model. A second publication, analysing the range of applicability of the so–called impulse approximation for Compton scattering from bound states is currently in preparation [19].

This project has received funding from the *European Unions Horizon 2020 research and innovation programme* under grant agreement No 654220.

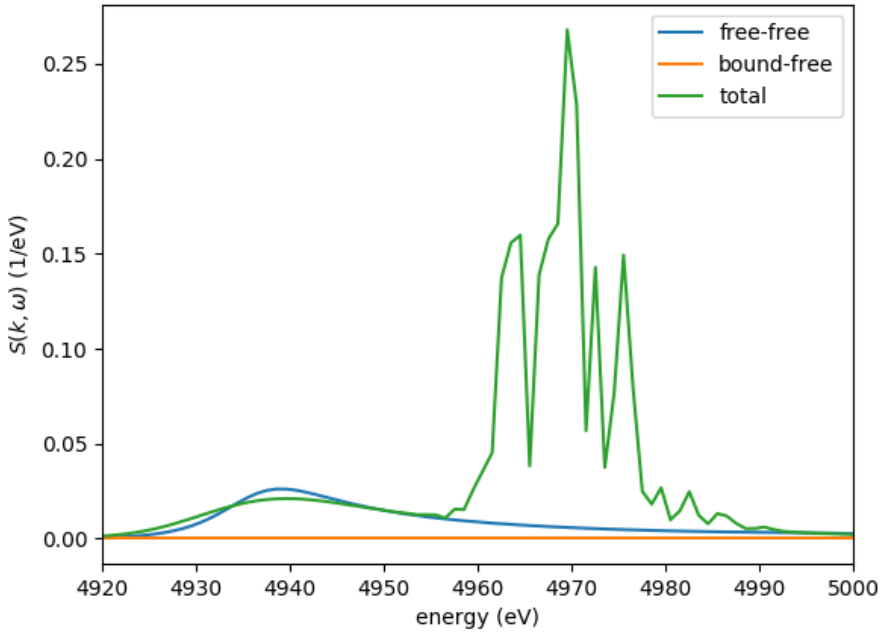

(a)

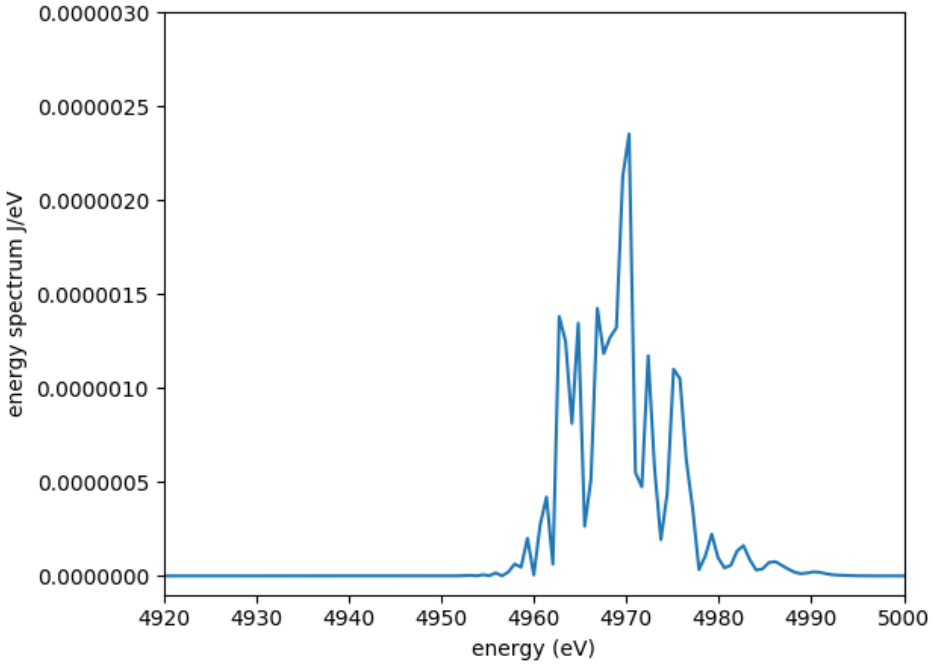

(b) SASE spectrum

Figure 9: (a) XRTS spectrum the total scattering as well as contributions from free–free and bound–free scattering. The source spectrum (b) determines the spectral shape of the elastic feature and smears our the inelastic features.

This project has received funding from the *European Unions Horizon 2020 research and innovation programme* under grant agreement No 654220.

6 Laser–plasma accelerator driven FEL source

Simulations of compact coherent x–ray sources based on the mechanism of electron laser wake-field acceleration couple particle–in–cell simulations to an FEL code. In our case, we use the Particle In Cell (PIC) code *PIConGPU* and the *Genesis* FEL code, both are publicly available under open source licenses. *PIConGPU* writes the particle and field data into a hdf5 file using the openPMD [27] meta-data standard. A file format conversion utility, which is part of *simex_platform* converts the PIC output to an electron distribution file (extension .dist) readable by *Genesis*.

This interface was used to investigate the possible route for the experimental realization of a laser plasma accelerator based coherent light source [13]. LPAs [14, 15, 16] have the potential to become the next generation of accelerator facilities reaching field gradients of the order of 100 GeV m^{-1}, i.e. up to three orders of magnitude higher than in conventional linear accelerators. This would reduce construction and operation costs by comparable orders of magnitude.

6.1 Start–to–end simulation of LPA based FELs

Our simulation setup is shown in Fig. 10; starting from electron beam generation from a laser plasma source to the generation of femtosecond and/or attosecond EUV/XUV pulse from the radiation undulator. In this scheme an intense 10 TW to 100 TW laser is focused onto a gas jet or a

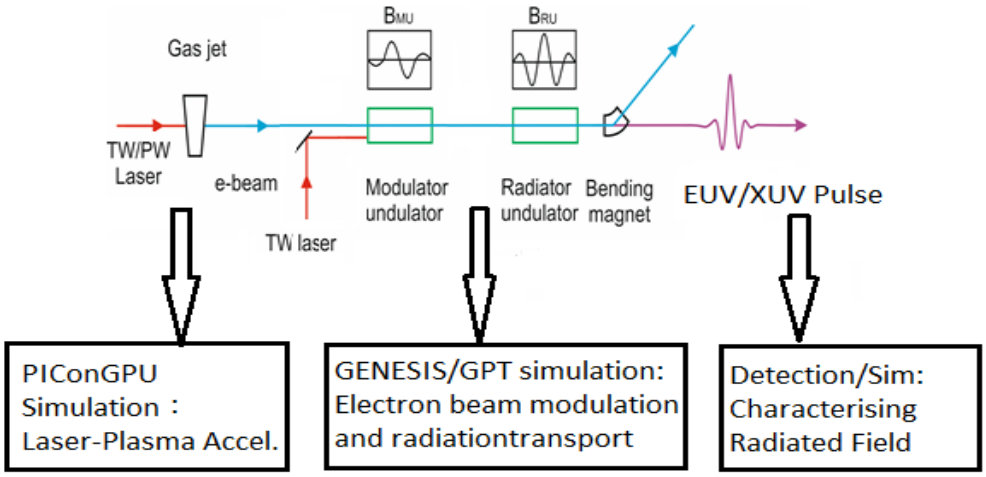

Figure 10: Scheme of LPA–FEL simulation

gas filled capillary for producing a relativistic electron beam. Initial energy spread of the electron beam of a LPA (1 to 5%) is typically much larger than that of a linear accelerator (about 0.05%), so reduction of the slice energy spread is necessary. The electron beam is sent through a modulator undulator (MU) together with a TW–power laser beam, where the interaction between the electrons, the magnetic field of the undulator and the electromagnetic field of the laser introduces a periodic energy modulation of the electrons. This energy modulation leads to the formation of nano–bunches (ultrashort electron layers). The nano–bunched electron beam then passes through a radiator undulator (RU) consisting of a single or a few periods and creates EUV/XUV pulses. The SIMEX setup (as shown in Fig. 10) for a LPA driven FEL utilizes the *PIConGPU* simulation code for electron beam generation using the LPA mechanism and further transportation of electron beam

This project has received funding from the *European Unions Horizon 2020 research and innovation programme* under grant agreement No 654220.

to the FEL simulation. We show a schema of the iterative SIMEX workflow in Fig. 11. We start by defining the initial laser–plasma parameters and initial conditions for *PIConGPU*. *PIConGPU* computes the 6D electron beam distributions at the rear side of the plasma in vacuum. The obtained electron beam distribution is transformed via a python script to a distribution file (.dist) for *GENESIS*). *GENESIS* calculates the electron beam dynamics induced by the magnetic field distribution. The output data file from *GENESIS* can be further post–processed to calculate and visualize the radiation field.

An online tutorial, demonstrating how to use the simulation capabilities and data format converters will be added to the *simex_platform* wiki pages soon. Generation of production simulation data for a realistic case study is currently hindered by the unavailability of sufficient computing resources. In order to simulate SIMEX for LPA driven FEL; we need adequate computing resources to run PIConGPU simulations for generation of high quality electron beam; a necessary condition for FEL radiation. At the moment, available GPUs for computation are short in numbers; subsequently we are unable to present the data in this report. A proposal for compute time at a high performance computing facility (e.g. within the PRACE) network) is currently being prepared.

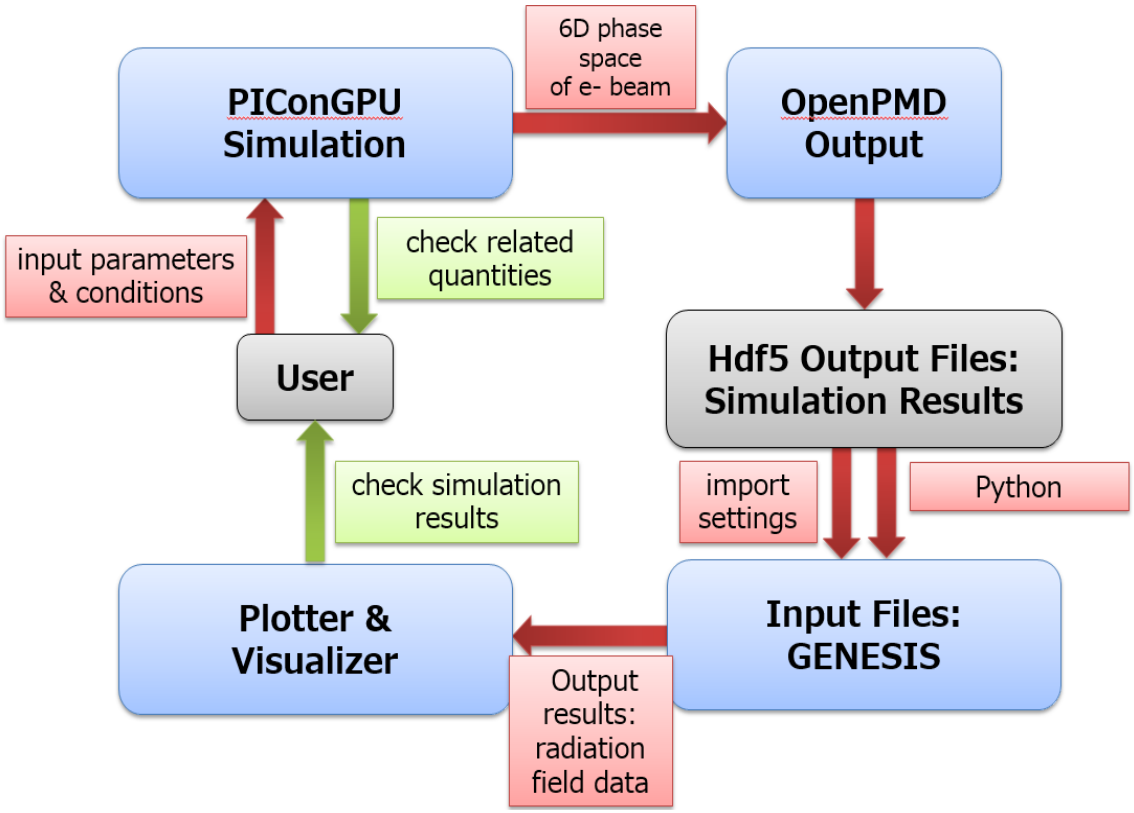

Figure 11: Layout for simulation setup and feedback loop

This project has received funding from the *European Unions Horizon 2020 research and innovation programme* under grant agreement No 654220.

6.2 Laser–plasma accelerator based single–cycle attosecond undulator source

In parallel, we have studied[1] the feasability of a LPA based coherent light source using experimental data for electron wakefield acceleration as input to the FEL simulation. The FEL simulation used the code *GPT* in this case. Details are discussed in Ref. [18].

Fig. 12 displays the simulated waveform (electric field as a function of time) of the generated attosecond pulse and the beam profile at 60 nm radiation wavelength. The temporal evolution was measured on the axis of highest intensity, marked by a cross in Fig. 12b. At other wavelengths, the shape of the attosecond pulses are nearly identical with the shape shown in Fig. 12a, showing that these pulses are Carrier–Envelope Phase (CEP) controlled [18].

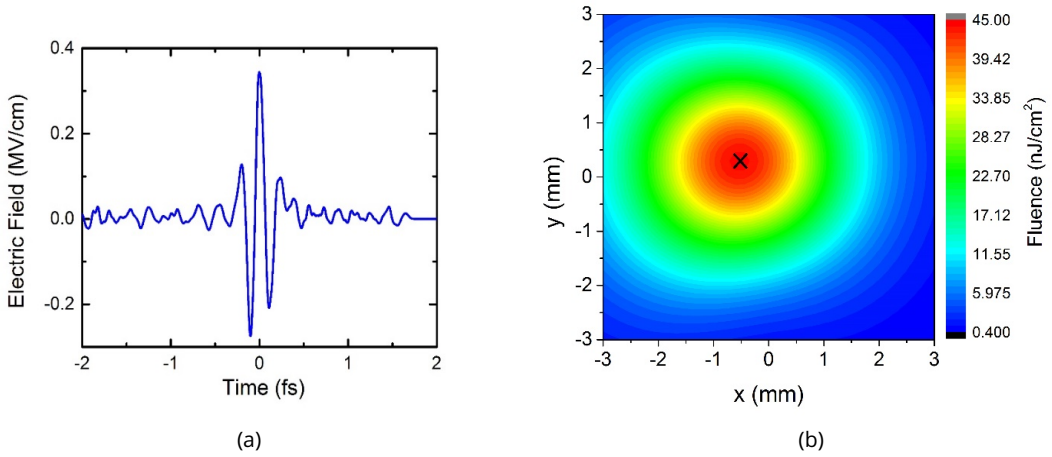

Figure 12: GPT Simulation Results: CEP–controlled Extreme Ultra–Violet (EUV) waveforms (left) and its spatial beam profile (right).

Journal articles

1. Fortmann-Grote, C., Buzmakov, A., Jurek, Z., Loh, N.-T. D., Samoylova, L., Santra, R., Schneidmiller, E. A., Tschentscher, T., Yakubov, S., Yoon, C. H., Yurkov, M. V., Ziaja-Motyka, B., and Mancuso, A. P., *Start-to-end simulation of single-particle imaging using ultra-short pulses at the European X-ray Free-Electron Laser*, *IUCrJ* **4,** 560–568 (2017).
2. Torchio, R., Occelli, F., Mathon, O., Sollier, A., Lescoute, E., Videau, L., Vinci, T., Benuzzi-Mounaix, A., Headspith, J., Helsby, W., Bland, S., Eakins, D., Chapman, D., Pascarelli, S., and Loubeyre, P., *Probing local and electronic structure in Warm Dense Matter: single pulse synchrotron x-ray absorption spectroscopy on shocked Fe*, *Sci. Rep.* **6,** 26402 (2016).
3. Kluge, T., Bussmann, M., Chung, H.-K., Gutt, C., Huang, L. G., Zacharias, M., Schramm, U., and Cowan, T. E., *Nanoscale femtosecond imaging of transient hot solid density plasmas with elemental and charge state sensitivity using resonant coherent diffraction*, *Physics of Plasmas* **23,** 033103 (2016).

[1] This study was performed in collaboration with T. Zoltan and Prof. Hebling, both at Pecs University, Hungary.

This project has received funding from the *European Unions Horizon 2020 research and innovation programme* under grant agreement No 654220.

4. Harmand, M. et al., *X-ray absorption spectroscopy of iron at multi megabar pressures in laser shock experiments*, *Phys. Rev. B* **92,** 024108 (2015).
5. Mazevet, S. et al., *Ab initio calculation of x-ray absorption of iron up to 3 Mbar and 8000 K*, *Phys. Rev. B* **89,** 111 (2014).
6. Fortmann, C., Bornath, T., Redmer, R., Reinholz, H., Röpke, G., Schwarz, V., and Thiele, R., *X-ray Thomson scattering cross-section in strongly correlated plasmas*, *Laser Part. Beams* **27,** 311 (2009).
7. Fortmann-Grote, C., *simex_platform version 0.3.3*, European Cluster of Advanced Laser Light-sources (EUCALL), <https://github.com/eucall-software/simex_platform/releases/tag/v0.3.3> (2017).
8. Colombier, J. P., Combis, P., Bonneau, F., Harzic, R. L., and Audouard, E., *Hydrodynamic simulations of metal ablation by femtosecond laser irradiation*, *Phys. Rev. B* **71,** 165406 (2005).
9. Rehr, J. J., Kas, J. J., Prange, M. P., Sorini, A. P., Takimoto, Y., and Vila, F., *Ab initio theory and calculations of X-ray spectra*, *Comptes Rendus Physique* **10,** 548–559 (2009).
10. White, T. A., Kirian, R. A., Martin, A. V., Aquila, A., Nass, K., Barty, A., and Chapman, H. N., *CrystFEL: a software suite for snapshot serial crystallography*, *Journal of Applied Crystallography* **45,** 335–341 (2012).
11. Glenzer, S. H., and Redmer, R., *X-ray Thomson scattering in high energy density plasmas*, *Rev. Mod. Phys.* **81,** 1625–1663 (2009).
12. Lee, H. J., Neumayer, P., Castor, J., Döppner, T., Falcone, R. W., Fortmann, C., Hammel, B. A., Kritcher, A. L., Landen, O. L., Lee, R. W., Meyerhofer, D. D., Munro, D. H., Redmer, R., Regan, S. P., Weber, S., and Glenzer, S. H., *X-Ray Thomson-Scattering Measurements of Density and Temperature in Shock-Compressed Beryllium*, *Phys. Rev. Lett.* **102,** 115001 (2009).
13. Emma, P., Bane, K., Cornacchia, M., Huang, Z., Schlarb, H., Stupakov, G., and Walz, D., *Phys. Rev. Lett.* **92,** 074801 (2004).
14. W. P. Leemans et al., *Nat. Phys.* **2,** 696 (2006).
15. E. Esarey and other, *Rev. Mod. Phys* **81,** 1229 (2009).
16. Tajima, T., and Dawson, J. M., *Phys. Rev. Lett* **43,** 43, 267 (1979).

Submitted articles

17. Rozmus, W., Brantov, A., Fortmann-Grote, C., Bychenkov, V. Y., and Glenzer, S., *Electrostatic fluctuations in collisional plasmas*, *submitted* (2017).
18. Tibai, Z., Tóth, G., Nagyváradi, A., Sharma, A., Mechler, M. I., Fülöp, J. A., Almási, G., and Hebling, J., *Laser-plasma accelerator based single-cycle attosecond undulator source*, *ArXiv e-prints*, <http://adsabs.harvard.edu/abs/2017arXiv170809384T> (2017).

Articles in preparation

19. Bell, F., Tschentscher, T., and Fortmann-Grote, C., *Compton profiles for plasmas of arbitrary degeneracy*, *in preparation* (2017).

This project has received funding from the *European Unions Horizon 2020 research and innovation programme* under grant agreement No 654220.

Project reports

20. Fortmann-Grote, C., *Milestone M4.2, First example simulation*, Project Milestone report, (European Cluster of Advanced Laser Lightsources (EUCALL), 2017), doi:10.5281/zenodo.896359, <https://dx.doi.org/10.5281/zenodo.896359>.
21. Fortmann-Grote, C., Andreev, A., Briggs, R., Bussmann, M., Huebl, A., Kluge, T., Pascarelli, S., Sharma, A., and Mancuso, A. P., *Milestone M4.1, Delivery of individual simulation modules and common interfaces for interoperability*, Project Milestone report, (European Cluster of Advanced Laser Lightsources (EUCALL), 2016), doi:10.5281/zenodo.896329, <https://dx.doi.org/10.5281/zenodo.896329>.
22. Fortmann-Grote, C., Andreev, A., Briggs, R., Bussmann, M., Huebl, A., Kluge, T., Pascarelli, S., Sharma, A., and Mancuso, A. P., *Deliverable D4.1, Design Report and Advanced Photon-Matter Simulation Software - Short Pulses*, Project Deliverable report, (European Cluster of Advanced Laser Lightsources (EUCALL), 2017), doi:10.5281/zenodo.890499, <https://dx.doi.org/10.5281/zenodo.890499>.
23. Fortmann-Grote, C., Andreev, A., Briggs, R., Bussmann, M., Huebl, A., Kluge, T., Pascarelli, S., Sharma, A., and Mancuso, A. P., *Deliverable D4.2, Design Report and Advanced Photon-Matter Simulation Software - Long Pulses*, Project Deliverable report, (European Cluster of Advanced Laser Lightsources (EUCALL), 2017), doi:10.5281/zenodo.890507, <https://dx.doi.org/10.5281/zenodo.890507>.
24. Fortmann-Grote, C., *Milestone M4.3, Simulations interoperable*, Project Milestone report, (European Cluster of Advanced Laser Lightsources (EUCALL), 2017), doi:10.5281/zenodo.998654, <https://dx.doi.org/10.5281/zenodo.998654>.
25. Fortmann-Grote, C., Garten, M., Huebl, A., Grund, A., Kluge, T., Bussmann, M., and Mancuso, A. P., *Deliverable D4.4, Simulated coherent scattering data from plasma and non–plasma samples*, Project Deliverable report, (European Cluster of Advanced Laser Lightsources (EUCALL), 2017), doi:10.5281/zenodo.998644, <https://dx.doi.org/10.5281/zenodo.998644>.

Datasets

26. Garten, M., Hübl, A., Grund, A., Fortmann-Grote, C., Kluge, T., and Bussmann, M., *ParaTAXIS X-ray Scattering Input & Output*, European Cluster of Advanced Laser Lightsources (EUCALL), <https://dx.doi.org/10.5281/zenodo.885033> (2017).
27. Hübl, A. *et al.*, *OpenPMD 1.0.0: A meta data standard for particle and mesh based data*, <https://dx.doi.org/10.5281/zenodo.33624> (2017).
28. Briggs, R., *Example OASYS workflow for the ID24 beamline of the European Synchrotron Radiation Facility*, European Cluster of Advanced Laser Light Sources (EUCALL), <https://dx.doi.org/10.5281/zenodo.886451> (2017).
29. Briggs, R., *Example input files and output data for 1D hydrodynamic simulations of shock compressed iron*, European Cluster of Advanced Laser Light Sources (EUCALL), <https://dx.doi.org/10.5281/zenodo.883106> (2017).

This project has received funding from the *European Unions Horizon 2020 research and innovation programme* under grant agreement No 654220.